

# Existence and Stability of Lanthanide–Main Group Element Multiple Bonds. New Paradigms in the Bonding of the 4f Elements. A DFT Study of $\text{Cp}_2\text{CeZ}$ ( $\text{Z} = \text{F}^+, \text{O}, \text{NH}, \text{CH}^-, \text{CH}_2$ ) and the Ligand Adduct $\text{Cp}_2\text{Ce}(\text{CH}_2)(\text{NH}_3)$

David L. Clark,<sup>\*,†</sup> John C. Gordon,<sup>\*,‡,§</sup> P. Jeffrey Hay,<sup>\*,⊥</sup> and Rinaldo Poli<sup>\*,||</sup>

*Nuclear Materials Technology Division and G. T. Seaborg Institute, Los Alamos National Laboratory, Mail Stop E500, Los Alamos, New Mexico 87545, Chemistry Division, Los Alamos National Laboratory, Mail Stop J514, Los Alamos, New Mexico 87545, Theoretical Division, Los Alamos National Laboratory, Mail Stop B268, Los Alamos, New Mexico 87545, and Laboratoire de Chimie de Coordination, UPR CNRS 8241, 205 Route de Narbonne, 31077 Toulouse Cedex, France*

Received August 9, 2005

We theoretically investigate the stability and nature of metal–ligand multiple bonding between the tetravalent lanthanide element cerium and a number of different ligand sets that commonly form metal–ligand multiple bonds in transition element chemistry. A comparison of electronic structure and bonding in a homologous series of bent metallocene complexes  $\text{Cp}_2\text{CeF}^+$ ,  $\text{Cp}_2\text{CeO}$ ,  $\text{Cp}_2\text{Ce}(\text{NH})$ ,  $\text{Cp}_2\text{Ce}(\text{CH}_2)$ , and  $\text{Cp}_2\text{Ce}(\text{CH})^-$  and the Lewis base adduct  $\text{Cp}_2\text{Ce}(\text{CH}_2)(\text{NH}_3)$  is presented. A direct comparison of bonding between  $\text{Cp}_2\text{CeO}$  and the transition element analogue  $\text{Cp}_2\text{HfO}$  is also discussed. We present an analysis of the Ce 4f and 5d orbital contribution to metal–ligand  $\sigma$  and  $\pi$  bonding interactions in  $\text{Cp}_2\text{CeZ}$  complexes and suggest the types of ligand systems that might support metal–ligand multiple bonds between 4f series and main group elements. In  $\text{Cp}_2\text{CeZ}$  systems, we find that the Ce–Cp interactions are best described as largely ionic in nature, whereas the Ce–Z interactions have a stronger covalent component. The optimized Ce–Z bonds are short, and the bonding analysis indicates the formation of metal–ligand  $\sigma$  and  $\pi$  bonds. Our theoretical studies suggest that a unique hybridization of Ce 4f, 5d, and 6p valence orbitals results in formation of very covalent metal–ligand  $\sigma$  bonds when compared to the transition element analogue. In contrast, the hybridization of Ce 4f and 5d valence orbitals in  $\pi$  bonds results in weaker metal–ligand  $\pi$  bonding than in the transition element analogue. The main result of the present computational study is the recognition that species with terminal multiple bonds between lanthanide ions (such as tetravalent cerium) and main group elements appear to be legitimate synthetic targets.

## Introduction

While metal–ligand multiply bonded carbene ( $\text{M}=\text{CHR}$ ), imido ( $\text{M}=\text{NR}$ ), and oxo ( $\text{M}=\text{O}$ ) complexes of the d-block elements have provided the basis for a large volume of research,<sup>1,2</sup> the lanthanide (Ln) elements have thus far defied all but a few attempts to prepare analogous multiply bonded derivatives. A few sparse reports of lanthanide compounds containing capping or bridging imido ligands have appeared, although detailed investigations of the nature of the bonding interactions

in these systems have not been addressed.<sup>3–8</sup> The paucity of such species appears unusual, since the related actinide (An) series displays numerous examples of complexes containing unsaturated  $\text{An}=\text{O}$ ,<sup>9–11</sup>  $\text{An}=\text{N}$ ,<sup>9,11–24</sup> and  $\text{An}=\text{P}^{25,26}$  linkages. Similarly, the

\* To whom correspondence should be addressed. E-mail: john.gordon@science.doe.gov.

† Nuclear Materials Technology Division and G. T. Seaborg Institute, Los Alamos National Laboratory.

‡ Chemistry Division, Los Alamos National Laboratory.

§ Currently on temporary assignment at: U.S. Department of Energy, Office of Basic Energy Sciences, Catalysis and Chemical Transformations Program, SC-14, 1000 Independence Ave., SW, Washington, DC 20585-1290.

⊥ Theoretical Division, Los Alamos National Laboratory.

|| Laboratoire de Chimie de Coordination.

(1) Nugent, W. A.; Mayer, J. M. *Metal–Ligand Multiple Bonds*; Wiley-Interscience: New York, 1988.

(2) Wigley, D. E. *Prog. Inorg. Chem.* **1994**, *42*, 239.

(3) Trifonov, A. A.; Bochkarev, M. N.; Schumann, H.; Loebel, J. *Angew. Chem., Int. Ed. Engl.* **1991**, *30*, 1149.

(4) Emelyanova, N. S.; Bochkarev, M. N.; Schumann, H.; Lebel, J.; Esser, L. *Koord. Khim.* **1994**, *20*, 789.

(5) Xie, Z.; Wang, S.; Yang, Q.; Mak, T. C. W. *Organometallics* **1999**, *18*, 1578.

(6) Wang, S.; Yang, Q.; Mak, T. C. W.; Xie, Z. *Organometallics* **1999**, *18*, 5511.

(7) Beetstra, D.; Meetsma, A.; Hessen, B.; Teuben, J. *Organometallics* **2003**, *22* (22), 4372–4374.

(8) Chan, H.-S.; Li, H.-W.; Xie, Z. *Chem. Commun.* **2002**, 652–653.

(9) Arney, D. S. J.; Burns, C. J. *J. Am. Chem. Soc.* **1993**, *115*, 9840.

(10) Duval, P. B.; Burns, C. J.; Buschmann, W. E.; Clark, D. L.; Morris, D. E.; Scott, B. L. *Inorg. Chem.* **2001**, *40*, 5491.

(11) Roussel, P.; Boaretto, R.; Kingsley, A. J.; Alcock, N. W.; Scott, P. J. *Chem. Soc., Dalton Trans.* **2002**, 1423.

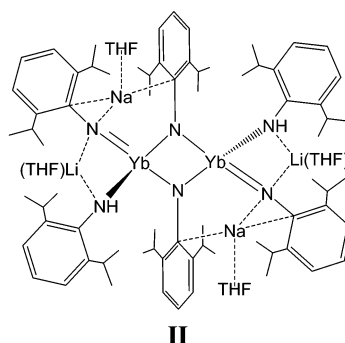
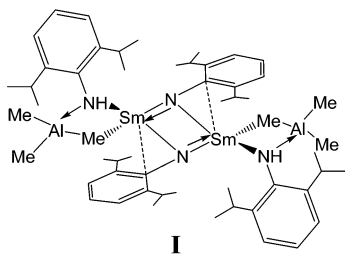
(12) Cramer, R. E.; Panchanatheswaran, K.; Gilje, J. W. *J. Am. Chem. Soc.* **1984**, *106*, 1853.

(13) Brennan, J. G.; Andersen, R. A. *J. Am. Chem. Soc.* **1985**, *107*, 514–516.

(14) Blake, P. C.; Lappert, M. F.; Taylor, R. G.; Atwood, J. L.; Zhang, H. *Inorg. Chim. Acta* **1987**, *139*, 13.

chemistry of uranium(VI) is dominated by complexes containing the linear trans dioxo, or uranyl, moiety ( $\text{UO}_2^{2+}$ ).<sup>27,28</sup> Therefore, whereas metal–ligand multiple bonds are well established for the 5f elements, their existence is less documented for the 4f elements and, as a result, a quantitative assessment of their strength and nature is notably absent. Some information on  $\text{Ln}=\text{Z}$  linkages with multiple-bond character (where  $\text{Z} = \text{C}$  or  $\text{N}$ ) is emerging from synthetic studies, as has been reviewed recently by Giesbrecht and Gordon.<sup>29</sup>

Recent work has highlighted rare examples of Ln imido compounds,  $[(\mu\text{-ArN})\text{Sm}(\mu\text{-NHAr})(\mu\text{-Me})\text{AlMe}_2]_2$  ( $\text{Ar} = 2,6\text{-}i\text{-Pr}_2\text{C}_6\text{H}_3$ ) (**I**),<sup>30</sup> which features bridging imido groups between two samarium atoms, and  $\{(\text{ArN})\text{-}(\text{ArNH})\text{Yb}(\mu\text{-ArN})\}_2[\text{Li}(\text{THF})][\text{Na}(\text{THF})]_2$  (**II**),<sup>8</sup> which features terminal imido groups stabilized by sodium or lithium interactions. For **I**, a theoretical analysis reveals the presence of  $\text{Sm}-\text{N} \pi$  bonding interactions involving the samarium valence 5d orbitals.<sup>30</sup> The 4f orbitals, on the other hand, do not seem to play a significant role in bonding in this compound.



While attempts are being made to generate compounds containing terminal lanthanide–main group

element multiple bonds,<sup>31,32</sup> it is reasonable to question whether such functional groups would be sufficiently stable to isolate and what the nature of these bonds would be (double, triple, purely ionic, highly covalent, etc.). For example, chemical bonding in lanthanide species is generally thought to be predominantly ionic on the basis of the premise that 4f orbitals are largely core-like and do not participate in bonding to any great extent.<sup>33–35</sup> Theoretical studies on the  $\text{Sm}_2(\mu\text{-NR})_2$  moiety in **I** indicated the presence of lanthanide element 5d orbital interactions, raising the question of what chemical conditions might promote the greater use of these orbitals in bonding. It seems reasonable to expect an increase in 5d orbital participation and greater covalency upon increasing the metal oxidation state. In this respect, the lanthanide elements are rather limited, with most lanthanides preferring the trivalent oxidation state. A notable exception is cerium, for which the +4 oxidation state is also possible.<sup>36–45</sup> The high propensity of lanthanide elements to achieve high coordination numbers requires the use of bulky ligands in order to prevent oligomerization (e.g., to achieve compounds such as **I**).<sup>46–49</sup> We therefore considered the bis(cyclopentadienyl)cerium(IV) system as a possible synthetic target for isolating a terminal metal–ligand multiple-bonding interaction and set out to perform computational analyses of  $\text{Cp}_2\text{CeZ}$  compounds (where  $\text{Z}$  is a divalent element or group) to assess the nature of chemical bonding and ascertain whether multiple metal–ligand bonding seemed feasible.

For the purpose of comparison, a calculation was also carried out on the related 5d compound  $\text{Cp}_2\text{HfO}$ . The present contribution will elaborate on the nature of the  $\text{Ce}^{\text{IV}}-\text{Z}$  bonds of various bond orders with  $\text{Z}$  varying

(15) Zalkin, A.; Brennan, J. G.; Andersen, R. A. *Acta Crystallogr.* **1988**, *C44*, 1553.

(16) Burns, C. J.; Smith, W. H.; Huffman, J. C.; Sattleberger, A. P. *J. Am. Chem. Soc.* **1990**, *112*, 3237.

(17) Arney, D. S. J.; Burns, C. J.; Smith, D. C. *J. Am. Chem. Soc.* **1992**, *114*, 10068–10069.

(18) Stewart, J. L.; Andersen, R. A. *New J. Chem.* **1995**, *19* (5–6), 587–595.

(19) Arney, D. S. J.; Burns, C. J. *J. Am. Chem. Soc.* **1995**, *117*, 9448.

(20) Hitchcock, P. B.; Lappert, M. F.; Liu, D. S. *J. Organomet. Chem.* **1995**, *488*, 241.

(21) Warner, B. J.; Scott, B. L.; Burns, C. J. *Angew. Chem., Int. Ed.* **1998**, *37*, 959.

(22) Peters, R. G.; Warner, B. P.; Burns, C. J. *J. Am. Chem. Soc.* **1999**, *121*, 5585.

(23) Diaconescu, P. L.; Arnold, P. L.; Baker, T. A.; Mindiola, D. J.; Cummins, C. C. *J. Am. Chem. Soc.* **2000**, *122* (25), 6108–6109.

(24) Kiplinger, J. L.; Morris, D. E.; Scott, B. L.; Burns, C. J. *Chem. Commun.* **2002** (30).

(25) Duttera, M. R.; Day, V. W.; Marks, T. J. *J. Am. Chem. Soc.* **1984**, *106*, 2907.

(26) Arney, D. S. J.; Schnabel, R. C.; Scott, B. C.; Burns, C. J. *J. Am. Chem. Soc.* **1996**, *118*, 6780.

(27) Katz, J. J.; Seaborg, G. T.; Morss, L. R. *The Chemistry of the Actinide Elements*; Chapman and Hall: London, 1986.

(28) Denning, R. G. *Struct. Bonding* **1992**, *79*, 215.

(29) Giesbrecht, G. R.; Gordon, J. C. *J. Chem. Soc., Dalton Trans.* **2004**, (16), 2387–2393.

(30) Gordon, J. C.; Giesbrecht, G. R.; Clark, D. L.; Hay, P. J.; Keogh, D. W.; Poli, R.; Scott, B. L.; Watkin, J. G. *Organometallics* **2002**, *21*, 4726–4734.

(31) Basuli, F.; Tomaszewski, J.; Huffman, J. C.; Mindiola, D. J. *Organometallics* **2003**, *22*, 4705.

(32) Knight, L. K.; Piers, W. E.; Fleurat-Lessard, P.; Parvez, M.; McDonald, R. *Organometallics* **2004**, *23*, 2087.

(33) Raymond, K. N.; Eigenbrot, C. W. *Acc. Chem. Res.* **1980**, *13*, 276.

(34) Maron, L.; Eisenstein, O. *J. Phys. Chem. A* **2000**, *104* (30), 7140–7143.

(35) Perrin, L.; Maron, L.; Eisenstein, O.; Lappert, M. F. *New J. Chem.* **2003**, *27* (1), 121–127.

(36) Kalsotra, B.; Multani, R.; Jain, B. *Isr. J. Chem.* **1971**, *9* (5), 569.

(37) Kalsotra, B.; Jain, B.; Multani, R. *J. Inorg. Nucl. Chem.* **1972**, *34* (7), 2265.

(38) Kapur, S.; Kalsotra, B.; Multani, R. *J. Chin. Chem. Soc.* **1972**, *19* (4), 197–202.

(39) Kapur, S.; Kalsotra, B.; Multani, R. *J. Inorg. Nucl. Chem.* **1973**, *35* (11), 3966–3968.

(40) Kalsotra, B.; Multani, R.; Jain, B. *J. Inorg. Nucl. Chem.* **1973**, *35* (1), 311–313.

(41) Kapur, S.; Kalsotra, B.; Multani, R.; Jain, B. *J. Inorg. Nucl. Chem.* **1973**, *35* (5), 1689–1691.

(42) Kapur, S.; Kalsotra, B.; Multani, R. *J. Inorg. Nucl. Chem.* **1974**, *36* (4), 932–934.

(43) Vij, P.; Bhalla, M.; Multani, R. *J. Chin. Chem. Soc.* **1978**, *25* (2), 95–98.

(44) Gulino, A.; Casarin, M.; Conticello, V.; Gaudiello, J.; Mauer-mann, H.; Fragala, I.; Marks, T. *Organometallics* **1988**, *7* (11), 2360–2364.

(45) Evans, W.; Deming, T.; Ziller, J. *Organometallics* **1989**, *8* (6), 1581–1583.

(46) Evans, W. J. *Adv. Organomet. Chem.* **1985**, *24*, 131.

(47) Schaverien, C. J. *Adv. Organomet. Chem.* **1994**, *36*, 283.

(48) Schumann, H.; Meese-Marktscheffel, J. A.; Esser, L. *Chem. Rev.* **1995**, *95*, 865.

(49) Anwander, R. *Top. Organomet. Chem.* **1999**, *2*, 1.

widely in electronegativity from F to C. The study includes an analysis of the Ce 4f and 5d orbital contribution to the bonding interaction and suggests the types of ligand systems that might support metal–ligand multiple bonds between lanthanide and main group elements.

### Computational Details

All calculations were carried out with the Gaussian98 program package,<sup>50</sup> using the B3LYP functional and employing a relativistic effective core potential (RECP) on the Ce atom. All calculations used the “small core” RECP in which the 4s<sup>2</sup> 4p<sup>6</sup> 4d<sup>10</sup> 5s<sup>2</sup> 5p<sup>6</sup> 6s<sup>2</sup> 5d<sup>1</sup> 4f<sup>1</sup> electrons were explicitly treated as “valence” electrons, with the remaining electrons replaced by the RECP,<sup>51</sup> and employing a (12s 11p 9d 8f) basis contracted to [5s 5p 4d 3f]. For the comparative calculation of Cp<sub>2</sub>HfO, the Hf atom was treated with the standard LANL2DZ basis set.<sup>52</sup> The 6-31G basis set was used for all ligand atoms. The calculations on the oxo compound were carried out in C<sub>2v</sub> symmetry, whereas all others were carried out in C<sub>1</sub> symmetry. The hydrogen atoms of the imido (NH) and carbyne (CH) ligands were placed off the symmetry axis in the starting geometries; they moved toward the axis during the optimization. The carbene (CH<sub>2</sub>) molecule was initially constructed with planar CeCH<sub>2</sub> and CCE<sub>1</sub>X<sub>2</sub> arrangements (X<sub>1</sub> and X<sub>2</sub> are the centroids of the two Cp rings) and with a 45° H–C–Ce–X dihedral angle. Frequency calculations verified that all optimized geometries correspond to true minima on the potential energy surface with no imaginary frequencies.

### Results and Discussion

**Theoretical Background.** Bis(cyclopentadienyl)cerium(IV) systems of the type Cp<sub>2</sub>CeZ<sup>+</sup> (Z = H, CH<sub>3</sub>, C<sub>2</sub>H<sub>5</sub>, SiH<sub>3</sub>) have been investigated in the Ziegler and the Maron and Eisenstein groups with a focus on olefin polymerization, C–H activation, and Si–H activation processes,<sup>53–56</sup> however, the issue of Ce–Z multiple bonding has not been previously addressed to the best of our knowledge. In most of the above-mentioned theoretical work the 4f electrons were not explicitly treated as valence electrons but rather incorporated into an effective core potential, as other older studies (mostly carried out on Ln(III) systems) had established negligible involvement of these electrons in Ln–Z bonding. Even for bis(cyclopentadienyl)Ln(II) systems, for which the 4f subshell will lie at higher energy, good agreement

with the experimental findings could be obtained by treating these electrons by a RECP.<sup>57</sup> These Ln(II) systems form adducts with  $\pi$ -acid ligands such as CO, N<sub>2</sub>, H<sub>2</sub>, olefins, and acetylenes, but the role of the 4f electrons was shown to be limited to electron–electron repulsion with the incoming ligand. This contrasts with the situation for Ce(C<sub>8</sub>H<sub>8</sub>)<sub>2</sub>, for which quantum chemical calculations showed the ground state is described by a Ce(III) ion in a 4f<sup>1</sup> configuration weakly coupled with an electron on the ligand.<sup>58,59</sup> Subsequent XANES experiments confirmed this description with the assignment of the oxidation state as Ce(III) in substituted cerocene complexes.<sup>60</sup> Previous theoretical calculations and photoelectron spectroscopy<sup>61,62</sup> had interpreted the electronic structure of cerocene in terms of a conventional closed shell Ce(IV) complex.

For our Ce(IV) systems the 4f orbitals may potentially be used, together with the 5d orbitals, to *accept* electron density. We have elected to use a small core basis set for the metal atom, because the main purpose of our investigation is to provide as accurate a description as possible of the potential for multiple bonding between the cerium atom and main group elements (F, O, N, C). Therefore, we have kept the entire fourth, fifth, and sixth shells in the valence set, with a small core consisting of the [Ar]3d<sup>10</sup> configuration (28 electrons). For the comparative study of compound Cp<sub>2</sub>HfO, the metal atom was treated, on the other hand, with a large core basis set, the entire fourth shell being placed in the core (total of 60 electrons). This is fully justified because, on one hand, the 4f subshell is filled and cannot be used to host additional  $\pi$  electron density coming from the ligands and, on the other hand, because the screening effects associated with the lanthanide contraction strongly stabilize this shell. The bonding for hafnium is essentially ensured by the valence 5d, 6s, and 6p orbitals, though the entire fifth shell orbitals and electrons were treated explicitly in the calculations.

**Optimized Geometries.** The model Cp<sub>2</sub>CeZ compounds with Z = F<sup>+</sup>, O, NH, and CH<sup>−</sup> adopt the C<sub>2v</sub>-symmetric geometry, which is typical of all compounds of this stoichiometry.<sup>63–65</sup> The relevant optimized geometric parameters are collected in Table 1. The Ce–Z distances are rather short. The distances increase in the order O < NH < CH<sup>−</sup>, following the order of decreasing electronegativity. There are no structurally characterized compounds with terminal Ce=O, Ce=NR, or Ce≡CR bonds to use as a reference for our calculated distances. The above trend is typical for isoelectronic series of d-block transition metal complexes, where the

(50) Frisch, M. J.; Trucks, G. W.; Schlegel, H. B.; Scuseria, G. E.; Robb, M. A.; Cheeseman, J. R.; Zakrzewski, V. G.; Montgomery, J., J. A.; Stratmann, R. E.; Burant, J. C.; Dapprich, S.; Millam, J. M.; Daniels, A. D.; Kudin, K. N.; Strain, M. C.; Farkas, O.; Tomasi, J.; Barone, V.; Cossi, M.; Cammi, R.; Mennucci, B.; Pomelli, C.; Adamo, C.; Clifford, S.; Ochterski, J.; Petersson, G. A.; Ayala, P. Y.; Cui, Q.; Morokuma, K.; Malick, D. K.; Rabuck, A. D.; Raghavachari, K.; Foresman, J. B.; Cioslowski, J.; Ortiz, J. V.; Baboul, A. G.; Stefanov, B. B.; Liu, G.; Liashenko, A.; Piskorz, P.; Komaromi, I.; Gomperts, R.; Martin, R. L.; Fox, D. J.; Keith, T.; Al-Laham, M. A.; Peng, C. Y.; Nanayakkara, A.; Gonzalez, C.; Challacombe, M.; Gill, P. M. W.; Johnson, B.; Chen, W.; Wong, M. W.; Andres, J. L.; Gonzalez, C.; Head-Gordon, M.; Replogle, E. S.; Pople, J. A. *Gaussian 98, Revision A.9*; Gaussian, Inc.: Pittsburgh, PA, 1998.

(51) Dolg, M.; Stoll, H.; Preuss, H. *J. Chem. Phys.* **1989**, *90* (3), 1730–1734.

(52) Hay, P. J.; Wadt, W. R. *J. Chem. Phys.* **1985**, *82*, 299–310.

(53) Margl, P.; Deng, L.; Ziegler, T. *Organometallics* **1998**, *17*, 933–946.

(54) Margl, P.; Deng, L.; Ziegler, T. *J. Am. Chem. Soc.* **1998**, *120*, 5517–5525.

(55) Perrin, L.; Maron, L.; Eisenstein, O. *Inorg. Chem.* **2002**, *41* (17), 4355–4362.

(56) Maron, L.; Perrin, L.; Eisenstein, O. *J. Chem. Soc., Dalton Trans.* **2002**, (4), 534–539.

(57) Perrin, L.; Maron, L.; Eisenstein, O.; Schwartz, D.; Burns, C.; Andersen, R. *Organometallics* **2003**, *22* (26), 5447–5453.

(58) Dolg, M.; Fulde, P.; Kuechle, W.; Neumann, C. S.; Stoll, H. *J. Chem. Phys.* **1991**, *94* (4), 3011–17.

(59) Dolg, M.; Fulde, P.; Stoll, H.; Preuss, H.; Chang, A.; Pitzer, R. M. *J. Chem. Phys.* **1995**, *103* (1, 2, 3), 71–82.

(60) Edelstein, N. M.; Allen, P. G.; Bucher, J. J.; Shuh, D. K.; Sofield, C. D.; Kaltsoyannis, N.; Maunder, G. H.; Russo, M. R.; Sella, A. J. *Am. Chem. Soc.* **1996**, *118* (51), 13115–13116.

(61) Rösch, N.; Streitwieser, A. *J. Am. Chem. Soc.* **1983**, *105* (25), 7237–7240.

(62) Rösch, N. *Inorg. Chim. Acta* **1984**, *94* (6), 297–299.

(63) Lauher, J. W.; Hoffmann, R. *J. Am. Chem. Soc.* **1976**, *98*, 1729–1742.

(64) Albright, T. A.; Burdett, J. K.; Whangbo, M. H. *Orbital Interactions in Chemistry*; J. Wiley & Sons: New York, 1985.

(65) Collman, J. P.; Hegedus, L. S.; Norton, J. R.; Finke, R. G. *Principles and Applications of Organotransition Metal Chemistry*; University Science Books: Mill Valley, CA, 1987.



**Table 1.** Selected DFT-Optimized Bond Distances (Å) and Angles (deg) for Cp<sub>2</sub>CeZ

	Z =					
	F <sup>+</sup>	O	NH	CH <sup>-</sup>	CH <sub>2</sub>	CH <sub>2</sub> (NH <sub>3</sub> ) <sup>b</sup>
Ce–CNT <sup>a</sup>	2.483	2.571	2.570	2.687	2.569	2.574
					2.539	2.584
Ce–Z	2.029	1.814	1.925	2.000	2.127	2.150
Z–H <sub>ax</sub>			1.025	1.114	1.097	1.098
Z–H <sub>eq</sub>					1.124	1.125
Ce···H <sub>eq</sub>					2.481	2.504
CNT–Ce–CNT'	125.8	124.6	125.4	125.5	131.7	130.0
CNT–Ce–Z	117.1	117.7	117.3	117.3	119.6	113.8
					106.9	107.3
Ce–Z–H <sub>ax</sub>			180.0	180.0	154.0	155.2
Ce–Z–H <sub>eq</sub>					94.4	94.6
H <sub>ax</sub> –Z–H <sub>eq</sub>					110.6	110.1

<sup>a</sup> CNT = Cp ring centroid. <sup>b</sup> Other relevant parameters: Ce–N = 2.650 Å; CNT–Ce–N = 103.8° and 100.5°; N–Ce–Z = 94.0°.

metal–ligand bond is expected to be more covalent in nature.<sup>1</sup> Using four-coordinate Mo compounds as an example, we note that Mo–O = 1.699(3) and 1.704(3) Å (av) in MoO<sub>2</sub>(2,4,6-Me<sub>3</sub>C<sub>6</sub>H<sub>2</sub>)<sub>2</sub><sup>66</sup> and MoO<sub>2</sub>(O-2,6-Me<sub>2</sub>C<sub>6</sub>H<sub>3</sub>)<sub>2</sub>,<sup>67</sup> Mo–N = 1.737(7) Å in Mo(N-2,6-Pr<sup>i</sup>-C<sub>6</sub>H<sub>3</sub>)(CHCMe<sub>2</sub>Ph)[BINA(N-Pr<sup>i</sup>)<sub>2</sub>],<sup>68</sup> and Mo–C = 1.754(6) Å in Mo(OAd)<sub>3</sub>(CCH<sub>2</sub>SiMe<sub>3</sub>).<sup>69</sup> In contrast, for our Cp<sub>2</sub>CeZ models, the longest Ce–Z distance is exhibited by the more electronegative fluorine atom (2.029 Å). For comparison, the Ce–F distance is 2.182(2) Å in [NH<sub>3</sub>-CH<sub>2</sub>CH<sub>2</sub>NH<sub>3</sub>][Ce<sub>2</sub>F<sub>10</sub>],<sup>70</sup> which, to the best of our knowledge, is the only crystallographically characterized compound containing a *terminal* Ce(IV)–F bond. The consideration of these distances as purely ionic would lead to the prediction of completely different distances and trends. Thus, when considering the accepted ionic radii of Ce<sup>4+</sup> (1.01 Å, from hexacoordinated compounds), F<sup>-</sup> (1.36 Å), O<sup>2-</sup> (1.40 Å), and N<sup>3-</sup> (1.71 Å), the predicted distances would be 2.37 Å for Ce–F, 2.41 Å for Ce–O, and 2.72 Å for Ce–N. In our interpretation, the extensive bond shortening, especially for Z = O and N, is a sign of significant covalent interaction in the corresponding bonds. The smaller shortening of the Ce–F distance, resulting in a Ce–F bond longer than the Ce–O bond, is therefore indicating a larger ionic component in the former bond, as one would expect. The Ce–Z bonding will be discussed in more detail later in light of the electronic structure analysis.

The distances between the Ce atom and the cyclopentadienyl centroids are rather long and markedly depend on the charge of the complex: longer (2.69 Å) for the anionic complex, shorter for the cationic one (2.48 Å), and intermediate for the two neutral molecules (2.57 Å). This trend follows what is experimentally established for cyclopentadienyl compounds of Ce(III): 2.561 Å for the anionic [Cp<sub>2</sub>CeCl<sub>2</sub>]<sup>-</sup>,<sup>71</sup> 2.538 (av), 2.521, 2.518 (av), and 2.533 Å for the neutral [(C<sub>5</sub>H<sub>3</sub>Bu<sub>2</sub>)<sub>2</sub>Ce(μ-H)]<sub>2</sub>,<sup>72</sup>

(66) Djafri, F.; Lai, R.; Pierrot, M. *Acta Crystallogr., Sect. C: Cryst. Struct. Commun.* **1989**, *45* (PR), 585–587.

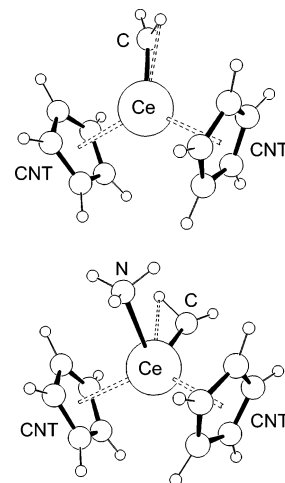
(67) Hanna, T.; Incarvito, C.; Rheingold, A. *Inorg. Chem.* **2000**, *39* (4), 630.

(68) Jamieson, J.; Schrock, R.; Davis, W.; Bonitatebus, P.; Zhu, S.; Hoveyda, A. *Organometallics* **2000**, *19* (5), 925–930.

(69) Tsai, Y.; Diaconescu, P.; Cummins, C. *Organometallics* **2000**, *19* (25), 5260–5262.

(70) Sykora, R.; Albrecht-Schmitt, T. *Chem. Mater.* **2001**, *13* (12), 4399–4401.

(71) Rausch, M.; Moriarty, K.; Atwood, J.; Weeks, J.; Hunter, W.; Brittain, H. *Organometallics* **1986**, *5* (6), 1281–1283.

**Figure 1.** ORTEP views of the optimized geometries for complexes Cp<sub>2</sub>Ce(CH<sub>2</sub>) and Cp<sub>2</sub>Ce(CH<sub>2</sub>)(NH<sub>3</sub>).

[(C<sub>5</sub>H<sub>3</sub>Bu<sup>t</sup>)<sub>2</sub>Ce(μ-Cl)]<sub>2</sub>,<sup>73</sup> Cp<sup>\*</sup><sub>2</sub>Ce[CH(SiMe<sub>3</sub>)<sub>2</sub>],<sup>74</sup> and [(C<sub>5</sub>H<sub>4</sub>Bu<sup>t</sup>)<sub>2</sub>Ce(μ-CH<sub>3</sub>)<sub>2</sub>],<sup>75</sup> respectively, and finally 2.470 (av) Å for the cationic [Cp<sup>\*</sup>Ce(THT)<sub>2</sub>]<sup>+</sup>.<sup>76</sup> This trend is consistent with a significant ionicity of the Ce–Cp bond, as will be analyzed in more detail in section (b). The angular parameters (CNT–Ce–CNT' and CTN–Ce–Z, where CNT is the centroid of the C<sub>5</sub> ring) are rather independent of the nature of Z.

The molecule with Z = CH<sub>2</sub> led to an optimized geometry with a distorted Ce=CH<sub>2</sub> moiety. This distortion is consistent with the establishment of an α-agostic interaction between one of the C–H bonds and the cerium atom (see Figure 1). The H<sub>ax</sub> atom is located nearly opposite the metal (Ce–C–H<sub>ax</sub> = 150°), whereas the H<sub>eq</sub> atom is drawn closer to the metal center (Ce···H = 2.481 Å; Ce–C–H<sub>eq</sub> = 94.4°). The sum of the angles at carbon (359°) indicates an essentially planar geometry at the C atom. The agostic interaction significantly lengthens the C–H bond. All these features are typical for α-agostic alkylidene moieties, as shown by experiment for electronically unsaturated d-block transition metal complexes<sup>1,77–85</sup> and by computational studies.<sup>86–89</sup> In the cerium compound, the plane of the

(72) Gunko, Y.; Bulychev, B.; Soloveichik, G.; Belsky, V. *J. Organomet. Chem.* **1992**, *424* (3), 289–300.

(73) Lobkovsky, E.; Gunko, Y.; Bulychev, B.; Belsky, V.; Soloveichik, G.; Antipin, M. *J. Organomet. Chem.* **1991**, *406* (3), 343–352.

(74) Heeres, H.; Renkema, J.; Booij, M.; Meetsma, A.; Teuben, J. *Organometallics* **1988**, *7* (12), 2495–2502.

(75) Stults, S.; Andersen, R.; Zalkin, A. *J. Organomet. Chem.* **1993**, *462* (1–2), 175–182.

(76) Heeres, H.; Meetsma, A.; Teuben, J. *J. Organomet. Chem.* **1991**, *414* (3), 351–359.

(77) Brookhart, M.; Green, M. L. H.; Wong, L.-L. *Progr. Inorg. Chem.* **1988**, *36*, 1–124.

(78) Churchill, M. R.; Youngs, W. J. *Inorg. Chem.* **1979**, *18* (7), 1930–1935.

(79) Messerle, L. W.; Jennische, P.; Schrock, R. R.; Stucky, G. J. *Am. Chem. Soc.* **1980**, *102* (22), 6744–6752.

(80) Wengrovius, J. H.; Schrock, R. R.; Churchill, M. R.; Wasserman, H. J. *J. Am. Chem. Soc.* **1982**, *104* (6), 1739–1740.

(81) Churchill, M. R.; Rheingold, A. L. *Inorg. Chem.* **1982**, *21* (4), 1357–1359.

(82) Mayr, A.; Asaro, M. F.; Kjelsberg, M. A.; Lee, K. S.; Van Engen, D. *Organometallics* **1987**, *6*, 432–434.

(83) Bryan, J. C.; Mayer, J. M. *J. Am. Chem. Soc.* **1987**, *109*, 7213–7214.

(84) Abbenhuis, H. C. L.; Feiken, N.; Grove, D. M.; Jastrzebski, J.; Kooijman, H.; Vandersluijs, P.; Smeets, W. J. J.; Spek, A. L.; Vankoten, G. *J. Am. Chem. Soc.* **1992**, *114* (25), 9773–9781.

(85) Kahlert, S.; Gorls, H.; Scholz, J. *Angew. Chem., Int. Ed.* **1998**, *37* (13–14), 1857–1861.

alkylidene moiety is neither parallel nor perpendicular to the CNT–Ce–CNT' plane, the angle between the two planes being 49.31°. The reasons for this choice will be analyzed in the electronic structure section. The Ce–C (methylene) bond length is longer than in the related methyne derivative, as expected. No Ce(IV) alkylidene complexes are available for comparison. The few reported lanthanide compounds with  $\pi$ -stabilized carbene ligands display much longer Ln–C distances, e.g., 2.552(4) Å in (C<sub>5</sub>Me<sub>4</sub>Et)<sub>2</sub>Yb(carbene),<sup>90</sup> 2.837(7) and 2.845(7) Å in Cp\*<sub>2</sub>Sm(carbene)<sub>2</sub>,<sup>91</sup> 2.663(4) Å in Eu(thd)<sub>3</sub>(carbene),<sup>91</sup> and 2.467(4) Å in Sm{C(Ph<sub>2</sub>PNSiMe<sub>3</sub>)<sub>2</sub>- $\kappa^3$ C,N,N'}(NCy<sub>2</sub>)(THF)}<sup>92</sup> (thd = 2,2,6,6-tetramethylheptane-3,5-dionato; carbene = 1,3-dimethylimidazolin-2-ylidene or 1,3,4,5-tetramethylimidazolin-2-ylidene).

The molecule that is obtained by addition of a neutral base (NH<sub>3</sub>) to the alkylidene complex Cp<sub>2</sub>Ce(CH<sub>2</sub>) leads to an optimized geometry where the two Cp, the CH<sub>2</sub>, and the NH<sub>3</sub> ligands occupy the expected positions (see Figure 1). It is noteworthy that the methylene ligand adopts a configuration that is essentially identical to that in the NH<sub>3</sub>-free complex, still featuring an  $\alpha$ -agostic interaction. This was unexpected because it formally corresponds to a 20-electron configuration for the metal center when counting the 12 electrons of the two Cp ligands, the two electrons of NH<sub>3</sub>, the four electrons of the M=CH<sub>2</sub> bond ( $\sigma + \pi$ ), and the two electrons of the agostically interacting C–H bond. Structures of isoelectronic tetravalent group 4 transition metals do not appear to be available, but the isostructural d<sup>0</sup> tantalocene derivative Cp<sub>2</sub>Ta(=CHPh)(CH<sub>2</sub>Ph) clearly shows a related structure with a parallel alkylidene ligand, a planar carbon atom, and no agostic interaction (i.e., a formal electron count of 18).<sup>93</sup> The reasons for this unexpected structural feature will be examined in a later section.

The NH<sub>3</sub> addition to the methylene complex does not significantly perturb the structure. The angle between the CeCH<sub>2</sub> plane and the CNT–Ce–CNT' plane is 39.95°. All other optimized parameters are remarkably close to those of the NH<sub>3</sub>-free molecule (see Table 1). The amine Ce–N distance of 2.650 Å is quite close to those experimentally determined for Ce(IV)-amine complexes: 2.624(7) Å in Ce[OCH(CF<sub>3</sub>)<sub>2</sub>]<sub>4</sub>(Me<sub>2</sub>NCH<sub>2</sub>CH<sub>2</sub>NMe<sub>2</sub>),<sup>94</sup> 2.687(5) and 2.785(5) Å in [Ce(OPr<sup>i</sup>)<sub>3</sub>(CCH<sub>2</sub>CH<sub>2</sub>N(Me)CH<sub>2</sub>CH<sub>2</sub>NMe<sub>2</sub>)]<sub>2</sub>,<sup>95</sup> and 2.699(5) Å in CeI-[(Bu<sup>t</sup>Me<sub>2</sub>SiNCH<sub>2</sub>CH<sub>2</sub>)<sub>3</sub>N].<sup>96</sup> For comparison, the tris-

(cyclopentadienyl) derivative of Ce(III), (C<sub>5</sub>H<sub>4</sub>Me)<sub>3</sub>Ce-[N(CH<sub>2</sub>CH<sub>2</sub>)<sub>3</sub>CH], has a slightly longer distance of 2.789(3) Å.<sup>97</sup> With respect to the fluoro, oxo, imido, and methyne complexes, the two methylene molecules show (counterintuitively) a slight opening of the CNT–Ce–CNT' angle. The Ce–CNT distances are close to those of the neutral oxo and imido complexes.

The comparative calculation on the Cp<sub>2</sub>HfO model also gives the expected bent metallocene structure, with Hf–O and Hf–CNT distances of 1.798 and 2.291 Å, respectively, and a CNT–Hf–CNT' angle of 129.28°. The calculated Hf–O distance is only slightly shorter than the calculated Ce–O bond distance in the homologous compound ( $\Delta = 0.016$  Å), while the ionic radius of Hf<sup>4+</sup> (0.81 Å) is much smaller than that of Ce<sup>4+</sup> ( $\Delta = 0.20$  Å), reflecting the lanthanide contraction. This is another indication of covalence for the Ce–O bond. The Hf–CNT distance, on the other hand, is much shorter than the Ce–CNT distance in Cp<sub>2</sub>CeO ( $\Delta = 0.280$  Å). A possible interpretation of this phenomenon is provided in the electronic structure section.

**Electronic Structure of the Fluoro, Oxo, Imido, and Methyne Complexes.** The most significant Kohn–Sham orbitals derived from the DFT calculations on the optimized C<sub>2v</sub>-symmetric Cp<sub>2</sub>CeZ molecules (Z = F<sup>+</sup>, O, NH, CH<sup>-</sup>) and those of the related Cp<sub>2</sub>Ce<sup>2+</sup> parent species are shown in the energy level diagram of Figure 2. The analysis of these orbitals in terms of atomic orbital contributions is reported in Table 2, Table 3, Table 4, and Table 5 for the fluoro, oxo, imido, and methyne compounds, respectively. The tables also report the orbital energies and symmetry labels. A direct relationship between the Kohn–Sham orbitals and the MOs deriving from an ab initio Hartree–Fock-based approach has been discussed.<sup>98</sup> Thus, the DFT-derived Kohn–Sham orbitals also provide a description of chemical bonding that is meaningful to the trained eyes of the experimental chemist. It is useful to start our analysis with a reminder of the well-investigated Cp<sub>2</sub>MZ electronic structure when M is a d-block transition metal.<sup>63,64</sup>

**(a) The [Cp<sub>2</sub>Ce]<sup>2+</sup> and [Cp<sub>2</sub>Hf]<sup>2+</sup> Fragments.** For a traditional d-block transition element, a bent metallocene fragment is characterized by six M–Cp orbital interactions, two of  $\sigma$  type (the in- and out-of-phase combinations of the Huckel-type  $\pi_1$  orbitals with the appropriate metal accepting orbitals) and four of  $\pi$  type (related combinations of the  $\pi_2$  and  $\pi_3$  Huckel orbitals). This leaves three low-energy metal orbitals available (1a<sub>1</sub>, b<sub>1</sub>, and 2a<sub>1</sub>, following the C<sub>2v</sub> symmetry labels) to establish further interactions with the orbitals of the Z ligand placed in the wedge plane.<sup>64</sup> In addition, the metal d<sub>yz</sub> orbital (of b<sub>2</sub> symmetry) establishes only a weak M–Cp  $\pi$  interaction when the metallocene bending is substantial. Thus, the antibonding component, which is mostly metal-based, is only slightly destabilized. The shape of these four well-known frontier orbitals, as obtained for the [Cp<sub>2</sub>Hf]<sup>2+</sup> ion, are shown in Figure 3. When M is an f-block element, however, the situation is further complicated by the presence of the f orbitals. For the Cp<sub>2</sub>Ce<sup>2+</sup> fragment, the 4f orbitals

(86) Cauchy, D.; Volatron, F.; Jean, Y. *New J. Chem.* **1994**, *18* (2), 191–196.

(87) Cauchy, D.; Eisenstein, O.; Jean, Y.; Volatron, F. *New J. Chem.* **1994**, *18* (6), 687–691.

(88) Fox, H. H.; Schofield, M. H.; Schrock, R. R. *Organometallics* **1994**, *13* (7), 2804–2815.

(89) Wu, Y. D.; Peng, Z. H. *J. Am. Chem. Soc.* **1997**, *119* (34), 8043–8049.

(90) Schumann, H.; Glanz, M.; Winterfeld, J.; Hemling, H.; Kuhn, N.; Kratz, T. *Angew. Chem., Int. Ed. Engl.* **1994**, *33* (17), 1733–1734.

(91) Arduengo, A.; Tamm, M.; Mclain, S.; Calabrese, J.; Davidson, F.; Marshall, W. *J. Am. Chem. Soc.* **1994**, *116* (17), 7927–7928.

(92) Aparna, K.; Ferguson, M.; Cavell, R. *J. Am. Chem. Soc.* **2000**, *122* (4), 726–727.

(93) Schrock, R. R.; Messerle, L. W.; Wood, C. D.; Guggenberger, L. *J. Am. Chem. Soc.* **1978**, *100* (12), 3793–3800.

(94) Daniele, S.; Hubert-Pfalzgraf, L.; Perrin, M. *Polyhedron* **2002**, *21* (20), 1985–1990.

(95) Hubert-Pfalzgraf, L.; Elkhokh, N.; Daran, J.-C. *Polyhedron* **1992**, *11* (1), 59–63.

(96) Morton, C.; Alcock, N.; Lees, M.; Munslow, I.; Sanders, C.; Scott, P. *J. Am. Chem. Soc.* **1999**, *121* (48), 11255–11256.

(97) Brennan, J.; Stults, S.; Andersen, R.; Zalkin, A. *Organometallics* **1988**, *7* (6), 1329–1334.

(98) Stowasser, R.; Hoffmann, R. *J. Am. Chem. Soc.* **1999**, *121*, 3414–3420.

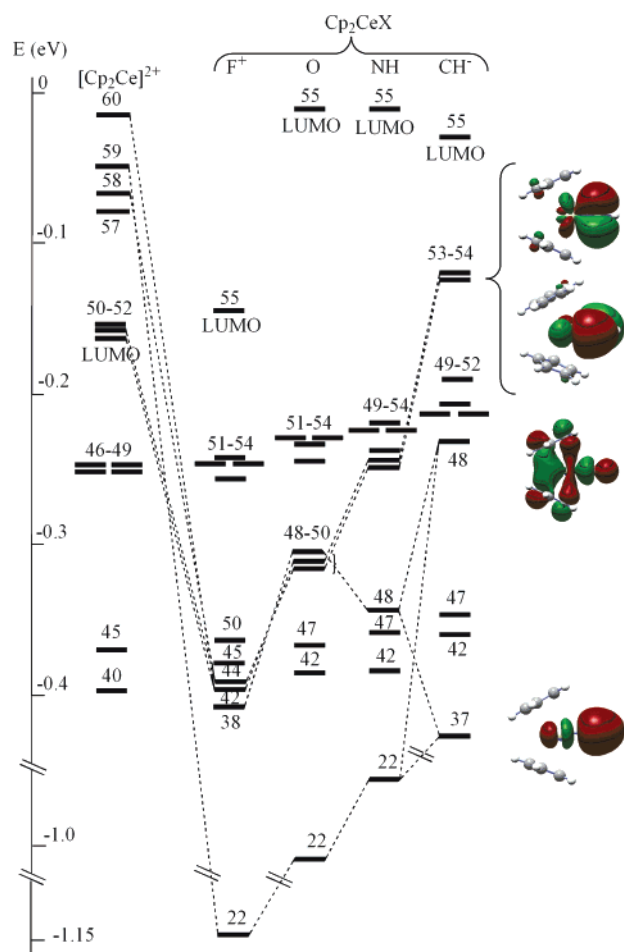


**Figure 2.** Energy diagram of the Kohn–Sham orbitals for the optimized  $\text{Cp}_2\text{CeZ}$  structures ( $Z = \text{F}^+, \text{O}, \text{NH}, \text{CH}^-$ ) and the frozen  $\text{Cp}_2\text{Ce}^{2+}$  moiety (geometry taken from the optimized oxo compound). The energy scaling [ $+0.305$  eV for  $\text{Cp}_2\text{Ce}^{2+}$ ,  $+0.161$  for  $\text{Cp}_2\text{CeF}^+$ , and  $-0.130$  eV for  $\text{Cp}_2\text{Ce}(\text{CH})^-$ ] is done as to maintain the C–C and C–H based orbitals of the Cp rings at constant energy (see text). The representative orbital contour plots shown refer to the calculation with  $Z = \text{CH}^-$ .

**Table 2.** Percent Atomic Orbital Contribution to the MOs of  $\text{Cp}_2\text{CeF}^+$

MO	$E$ (eV)	Ce				F		C
		s	p	d	f	s	p	tot
55 (LUMO), $b_1$	-0.306	0.0	1.3	0.5	87.6	0.0	0.6	10.4
54 (Ce–Cp $\pi$ ), $b_2$	-0.404	0.0	1.0	5.6	23.6	0.0	0.1	69.6
53 (Ce–Cp $\pi$ ), $b_1$	-0.405	0.0	4.4	4.2	12.6	0.0	0.4	78.2
52 (Ce–Cp $\pi$ ), $a_1$	-0.407	0.0	3.1	8.1	3.3	0.0	2.2	83.2
51 (Ce–Cp $\pi$ ), $a_2$	-0.418	0.0	0.0	17.0	4.1	0.0	0.0	78.6
50 (Ce–Cp $\sigma$ ), $b_2$	-0.524	0.0	7.6	2.3	0.3	0.0	6.5	65.6
45 (Ce–Cp $\sigma$ ), $a_1$	-0.545	4.6	3.0	6.1	1.2	0.1	24.7	57.2
44 (Ce–F $\pi$ ), $b_1$	-0.556	0.0	0.6	4.3	2.8	0.1	61.8	21.0
42 (Ce–F $\pi$ ), $b_2$	-0.559	0.0	0.5	3.8	4.2	0.0	52.1	27.0
38 (F 2p), $a_1$	-0.566	1.1	1.0	5.1	1.4	0.5	33.8	39.6
22 (F 2s), $a_1$	-1.309	1.0	8.8	0.2	0.0	88.6	1.7	0.0

fall in an energy range near that of the four metallocene frontier orbitals, d–f mixing occurs, and we obtain seven relevant metallocene frontier orbitals for the 4f  $\text{Cp}_2\text{M}$  fragment. Three d–f combinations of type  $a_1$  (mostly using the  $2a_1$  d-type orbital, cf. no. 43 for  $\text{Cp}_2\text{Hf}^{2+}$ ),  $b_1$ , and  $b_2$  give rise to in-phase hybrids (whose character is predominantly f) at lower energy (orbitals nos. 50–52) and the corresponding out-of-phase hybrids (predominantly d) at higher energy (orbitals 58, 59, and 60).

**Table 3.** Percent Atomic Orbital Contribution to the MOs of  $\text{Cp}_2\text{CeO}$

MO	$E$ (eV)	Ce				O		C
		s	p	d	f	s	p	tot
55 (LUMO), $b_1$	-0.105	0.0	0.8	0.5	94.7	0.0	0.1	3.6
54 (Ce–Cp $\pi$ ), $b_2$	-0.228	0.0	0.7	2.9	10.9	0.0	0.7	84.6
53 (Ce–Cp $\pi$ ), $a_1$	-0.228	0.2	1.9	4.8	10.3	0.0	8.5	74.6
52 (Ce–Cp $\pi$ ), $b_1$	-0.232	0.0	5.3	1.6	5.0	0.0	1.8	86.6
51 (Ce–Cp $\pi$ ), $a_2$	-0.244	0.0	0.0	13.1	2.4	0.0	0.0	84.6
50 (Ce–O $\sigma$ ), $a_1$	-0.304	0.5	7.8	14.9	11.2	1.2	51.1	13.6
49 (Ce–O $\pi$ ), $b_2$	-0.310	0.0	2.8	10.8	7.9	0	71.1	7.4
48 (Ce–O $\pi$ ), $b_1$	-0.317	0.0	1.0	15.1	7.7	0.0	74.3	2.0
47 (Ce–Cp $\sigma$ ), $b_2$	-0.367	0.0	3.8	5.8	0.4	0.0	4.3	76.2
42 (Ce–Cp $\sigma$ ), $a_1$	-0.385	7.2	2.0	2.7	0.1	0.2	0.9	86.4
22 (Ce–O $\sigma$ ), $a_1$	-1.011	0.7	43.8	0.3	0.0	49.4	4.5	1.4

<sup>a</sup> One Ce–Cp  $\pi$  interaction and the O lone pair are slightly mixed in orbitals 53 and 50.

**Table 4.** Percent Atomic Orbital Contribution to the MOs of  $\text{Cp}_2\text{Ce}(\text{NH})$

MO	$E$ (eV)	Ce				N		C
		s	p	d	f	s	p	tot
55 (LUMO), $b_1$	-0.098	0.0	1.2	0.0	94.1	0.0	0.6	3.6
54 (Ce–Cp $\pi$ ), $b_2$	-0.220	0.0	0.0	0.3	20.4	0.0	11.6	67.2
53 (Ce–Cp $\pi$ ), $b_1$	-0.223	0.0	6.3	0.1	8.5	0.0	4.7	68.8
52 (Ce–Cp $\pi$ ), $a_1$	-0.227	0.0	3.2	4.5	2.3	1.3	2.4	85.0
51 (Ce–Cp $\pi$ ), $a_2$	-0.239	0.0	0.0	12.9	2.4	0.0	0.0	84.6
50 (Ce–N $\pi$ ), $b_2$	-0.242	0.0	2.6	16.5	5.3	0.0	57.2	18.6
49 (Ce–N $\pi$ ), $b_1$	-0.247	0.0	0.0	18.6	7.9	0.0	54.3	19.2
48 (N–H $\sigma$ ), $a_1$	-0.343	0.1	5.9	15.7	4.8	7.6	36.4	14.8
47 (Ce–Cp $\sigma$ ), $b_2$	-0.360	0.0	4.6	3.9	0.1	0.0	0.4	90.4
42 (Ce–Cp $\sigma$ ), $a_1$	-0.384	8.2	1.7	2.6	0.7	0.7	6.6	77.4
22 (Ce–N $\sigma$ ), $a_1$	-0.957	0.3	62.0	0.2	0.1	16.9	1.9	17.6

<sup>a</sup> One Ce–Cp  $\pi$  and the N–H  $\sigma$  interactions are slightly mixed in orbitals 52 and 48. Contribution from the imido H atom: 1.2% in orbital 52; 14.3% in orbital 48.

**Table 5.** Percent Atomic Orbital Contribution to the MOs of  $[\text{Cp}_2\text{Ce}(\text{CH})]^-$

MO	$E$ (eV)	Ce				C (carbyne)		C (Cp)
		s	p	d	f	s	p	tot
55 (LUMO), $a_1$	+0.096	44.4	0.0	39.4	8.2	1.2	0.9	5.4
54 (Ce–C $\pi$ ), $b_2$	+0.005	0.0	2.1	18.6	31.8	0.0	46.1	1.8
53 (Ce–C $\pi$ ), $b_1$	+0.003	0.0	0.5	27.4	14.2	0.0	51.5	2.0
52 (Ce–Cp $\pi$ ), $a_1$	-0.057	2.0	3.5	7.5	4.9	11.4	20.8	39.0
51 (Ce–Cp $\pi$ ), $b_2$	-0.076	0.0	0.9	4.5	1.5	0.0	0.9	92.2
50 (Ce–Cp $\pi$ ), $b_1$	-0.082	0.0	3.7	4.1	1.2	0.0	0.4	90.8
49 (Ce–Cp $\pi$ ), $a_2$	-0.088	0.0	0.0	9.4	1.2	0.0	0.0	89.6
48 (Ce–C $\sigma$ ), $a_1$	-0.103	1.1	1.9	18.1	1.3	4.5	12.5	53.4
47 (Ce–Cp $\sigma$ ), $b_2$	-0.217	0.0	3.1	2.4	0.1	0.0	0.1	94.4
42 (Ce–Cp $\sigma$ ), $a_1$	-0.234	4.5	1.1	1.7	0.3	0.0	0.8	86.8
37 (C–H $\sigma$ ), $a_1$	-0.347	2.3	3.0	2.8	0.6	52.1	7.9	0.2

<sup>a</sup> One Ce–Cp  $\pi$ , the Ce–C  $\sigma$ , and the C–H  $\sigma$  interactions are heavily mixed in orbitals 52, 48, and 37. Contribution from the carbyne H atom: 11.1% in orbital 52, 6.9% in orbital 48, and 30.9% in orbital 37.

Orbital 57 remains an essentially pure d orbital, corresponding to orbital no. 41 ( $1a_1$ ) of fragment  $\text{Cp}_2\text{Hf}^{2+}$ . The shapes of these seven  $\text{Cp}_2\text{Ce}^{2+}$  frontier orbitals are also shown in Figure 3. Orbitals nos. 53–56 are the four remaining 4f orbitals, which do not significantly mix with the d orbitals of the same symmetry types because of their very different nodal structure (small overlap). Thus, the  $\text{Cp}_2\text{Ce}^{2+}$  fragment has the potential to use both the high-energy orbitals (58–60) and the lower energy ones (50–52) to establish bonding interactions with the wedge Z group. This is a notable difference from the normal frontier orbitals of the  $\text{Cp}_2\text{M}$  fragment for a transition element.



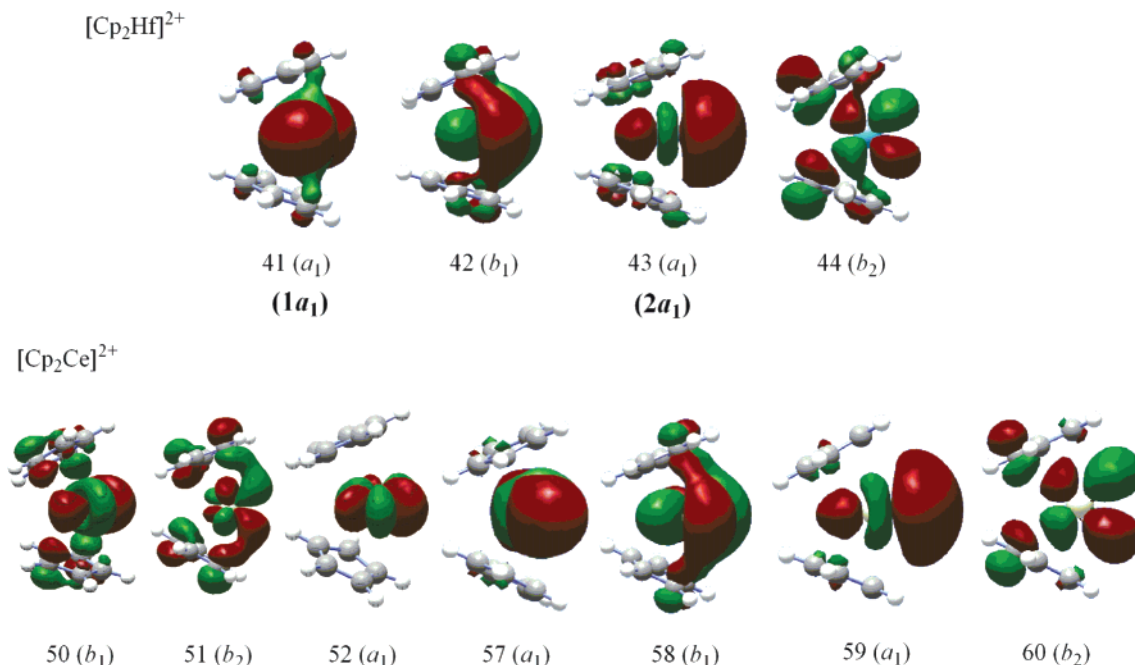


**Figure 3.** Shape of the relevant empty Kohn–Sham orbitals for the  $[Cp_2Hf]^{2+}$  and  $[Cp_2Ce]^{2+}$  ions. Orbitals nos. 41 and 43 for  $[Cp_2Hf]^{2+}$  refer to the combinations  $1a_1$  and  $2a_1$  of the  $Cp_2M$  fragment, respectively.<sup>64</sup>

The two Ce–Cp  $\sigma$  interactions in  $[Cp_2Ce]^{2+}$  (see Figure 2, MOs nos. 40 and 45) are found in the  $-0.4$  eV region, and the four  $\pi$  interactions (MOs nos. 46–49) are in the  $-0.25$  eV region after scaling the energies to account for the electrostatic effect of the double positive charge. The energy scaling for this ion, as well as for the positively charged fluoro complex and the negatively charged methyne complex that will be discussed later, was conveniently performed by using the C–C and C–H orbitals of the Cp ligands as an internal standard. In fact, these orbitals (not shown in Figure 2) are not affected by the nature of the Z substituent (nor by its absence) neither directly nor indirectly, since they have neither Z nor metal contribution, except for particular cases, which will be highlighted later.

**(b) Bonding between  $[Cp_2Ce]^{2+}$  and  $Z^{n-}$ .** Moving on to the  $Cp_2CeZ$  derivatives, each resulting MO diagram can be analyzed as the result of the interaction between the frontier  $Cp_2Ce^{2+}$  fragment orbitals and the available orbitals of the appropriate  $F^-$ ,  $O^{2-}$ ,  $NH^{2-}$ , and  $CH^{3-}$  unit, respectively. In each case, the Z group possesses three filled donor orbitals ( $1\sigma + 2\pi$ ), which match in symmetry with the empty in- and out-of-phase d–f hybrids of the  $Cp_2Ce^{2+}$  fragment. This interaction leads to formation of three new bonding orbitals ( $1\sigma$  and  $2\pi$  Ce–Z bonds). A fourth filled, noninteracting orbital (lone pair 2s for  $F^-$ ,  $O^{2-}$ , N–H  $\sigma$  bond for  $NH^{2-}$  and C–H  $\sigma$  bond for  $CH^{3-}$ ) is also introduced by the Z group. This noninteracting orbital is a basis for the same irreducible representation of the  $C_{2v}$  symmetry group as the Ce–Z  $\sigma$  bond ( $a_1$ ), which leads to a variable extent of mixing between the two as a function of the nature of Z. The Z donor atom (i.e., F, O, N, C) contributes to these two  $a_1$  orbitals with its s and  $p_\sigma$  atomic orbitals.

These four orbitals are highlighted by the dashed lines in Figure 2 and are depicted on the right of the Figure for Z =  $CH^-$  in descending energy: two Ce–Z  $\pi$  bonds (nos. 53 and 54), one Ce–Z  $\sigma$  bond (no. 48), and the C–H bond (no. 37). As one proceeds leftward on the

chart from Z =  $CH^-$  to  $F^+$ , the dashed lines indicate how these four orbitals correlate across the series. The Ce–Z  $\pi$  bonds correlate very straightforwardly, becoming nos. 42 and 44 for Z =  $F^+$ . The lowest  $\sigma$  orbital progressively becomes the Ce–N bond and then O 2s and F 2s lone pairs. The higher  $\sigma$  orbital in Figure 2 becomes the N–H bond, Ce–O bond, and Ce–F bond, although the latter is mostly made up of the F 2p lone pairs, in line with the expected strong polarity of this  $\sigma$  bond. Finally we note that one symmetry combination of the Ce–Cp  $\sigma$  bonds as well as one symmetry combination of the Ce–Cp  $\pi$  bonds both have  $a_1$  symmetry that can also mix with these two orbitals.

On going from  $F^+$  to  $CH^-$ , three different effects can be observed: (i) the energy of both  $\sigma$  orbitals sharply increases as the Z electronegativity decreases; (ii) there is an increasing degree of mixing between the two interactions; (iii) the Z contribution decreases and the Ce contribution increases. In particular, the lower energy orbital of these two MOs is a relatively pure Ce–Z  $\sigma$  bonding orbital and the Z contribution is predominantly s when Z =  $F^+$  and O (no. 22), but on going to Z = NH, a minor fraction of N–H  $\sigma$  bonding character mixes in (no. 22, 0.5% H contribution). On going further to Z =  $CH^-$ , the mixing increases further and the energy ordering of the two interactions is inverted, such that the lower energy combination (no. 37) has mostly C–H  $\sigma$  bonding character and the higher one (no. 48) has mostly Ce–C  $\sigma$  bonding character. In addition, the upper energy of these two MOs also features a significant degree of mixing with the Ce–Cp  $\sigma$  and Ce–Cp  $\pi$  bonding orbitals of the same symmetry, the greater degree of mixing being observed with the orbitals that are closest in energy: the Ce–Cp  $\sigma$  bonding orbital for Z =  $F^+$  and the Ce–Cp  $\pi$  bonding orbital for the methyne case.

The energy of the Ce–Z  $\pi$  bonding orbitals also sharply increases on going from  $F^+$  through O and NH to  $CH^-$ , accompanied by an increase of the Ce atomic

**Table 6.** NBO and Mulliken (in parentheses) Charge Analysis for  $\text{Cp}_2\text{CeZ}$  ( $\text{Z} = \text{F}^+$ ,  $\text{O}$ ,  $\text{NH}$ ,  $\text{CH}^-$ ,  $\text{CH}_2$ ), for  $\text{Cp}_2\text{Ce}(\text{CH}_2)(\text{NH}_3)$ , and for  $\text{Cp}_2\text{HfO}$ 

atom/group	Z = F <sup>+</sup>	Z = O	Z = NH	Z = CH <sup>-</sup>	Z = CH <sub>2</sub>	Z = CH <sub>2</sub> + NH <sub>3</sub>	atom	Cp <sub>2</sub> HfO
Ce	2.371 (0.743)	2.421 (0.666)	2.380 (0.718)	2.157 (0.114)	2.266 (0.480)	2.200 (0.466)	Hf	2.058 (0.822)
2 Cp	-0.746 (0.584)	-1.347 (-0.259)	-1.346 (-0.562)	-1.712 (-0.875)	-1.397 (-0.276)	-1.417 (-0.392)	2 Cp	-1.080 (-0.329)
F/O/N/C	-0.625 (-0.327)	-1.074 (-0.407)	-1.423 (-0.432)	-1.593 (-0.255)	-1.266 (-0.466)	-1.235 (-0.461)	O	-0.978 (-0.493)
H <sup>a</sup>	(-)	(-)	0.389 (0.274)	0.148 (0.016)	0.218 (0.137)	0.213 (0.123)		
H <sup>b</sup>	(-)	(-)	(-)	(-)	0.179 (0.125)	0.171 (0.110)		
Z (total)	-0.625 (-0.327)	-1.074 (-0.407)	-1.034 (-0.158)	-1.445 (-0.239)	-0.869 (-0.204)	-0.850 (-0.231)		

<sup>a</sup> Single H atom on the NH or CH<sup>-</sup> group; pseudoaxial H atom on the CH<sub>2</sub> group. <sup>b</sup> Pseudoequatorial H atom on the CH<sub>2</sub> group.

contribution and the corresponding decrease of the Z atomic contribution. In addition, like the Ce–Z  $\sigma$  interaction examined above, some mixing occurs with the Ce–Cp  $\pi$  interactions of appropriate symmetry. The mixing is strongest for the Z = NH molecule, where these orbitals are closest in energy. It is notable that the  $\pi_{||}$  interaction ( $b_2$  type) affords an equally stabilized bonding combination as the  $\pi_{\perp}$  interaction ( $b_1$  type), without significant interference from the Cp Hückel-type orbitals, whereas an antibonding interaction destabilizes the parent orbital (no. 60) in the precursor  $[\text{Cp}_2\text{Ce}]^{2+}$  fragment. The relative Ce:Z contribution in the Ce–Z  $\pi_{\perp}$  ( $b_2$ ) and  $\pi_{||}$  ( $b_1$ ) bonding orbitals changes with the nature of Z: the metal contribution increases and the Z contribution decreases on going from F<sup>+</sup> to CH<sup>-</sup>. This illustrates the increasing covalency of the Ce–Z bonds as the electronegativity of Z decreases. For Z = F<sup>+</sup>, in fact, these interactions can be described as prevalently ionic (see also the charge analysis below). For Z = CH<sup>-</sup>, these orbitals (nos. 53 and 54) have energies between those of the parent  $[\text{Cp}_2\text{Co}]^{2+}$  “d” (nos. 58–60) and “f” (nos. 50–52) orbitals.

The MOs describing the Ce–Cp  $\sigma$  interactions (45 and 50 for Z = F, 42 and 47 for all other systems) and the Ce–Cp  $\pi$  interactions (51–54 for Z = F<sup>+</sup>, O, and NH; 49–52 for Z = CH<sup>-</sup>) also show an energy increase as the Z electronegativity decreases. This change, however, is much less pronounced relative to that of the Ce–Z  $\sigma$  and  $\pi$  bonding orbitals. The reason for this is the relatively small metal participation in these orbitals (see Tables 2–5). These trends suggest that the Ce–Cp interactions are largely ionic in nature, whereas the Ce–Z interactions have a stronger covalent component, except perhaps for the fluoro complex. In a formal sense, these molecules could therefore be described as ionic bis-(cyclopentadienyl) derivatives of the  $[\text{CeO}]^{2+}$ ,  $[\text{CeNH}]^{2+}$ , and  $[\text{CeCH}]^+$  ions. This view is somewhat supported by the atomic charge analyses, *vide infra*.

The LUMO is an f orbital for the fluoro, oxo, and imido complexes, whereas it corresponds to the  $1a_1$  Cp<sub>2</sub>M fragment orbital for the carbyne complex. This inversion is caused by the greater influence that the effective metal charge has on the f orbitals than on the  $1a_1$  orbital. It is notable that most filled MOs for all systems exhibit a *significant f orbital participation*, especially the two orbitals describing the Ce–Z  $\pi$  interactions. This participation is particularly high (31.8%, or 60.6% of the overall metal contribution) for the  $\pi_{||}$  interaction in the carbyne complex (see Table 5). The reason for this

strong participation may be related to the efficient charge transfer from the Z ligand to the metal center (see NBO analysis below), which results in a concomitant rise in energy and a spatial expansion of the 4f orbital. The better energy match and the greater overlap with the Z donor orbitals favor a stronger interaction. This is a very different scenario than the typical bonding situation in Ln(III) chemistry, where the f orbital participation is indicated as negligible by the computations, even in the presence of less electronegative ligands, as in the case of trialkyls and tris(amido) compounds.<sup>34,35,99,100</sup>

**(c) Charge and Population Analyses.** The atomic charge and orbital population analyses were carried out by the standard Mulliken method as well as by the natural bond orbital (NBO)<sup>101</sup> method. In particular, NBO is known to provide a better description of weak and ionic interactions, whereas the Mulliken analysis tends to overemphasize covalency. The results of both analyses are shown in Table 6. In particular, the NBO analysis assigns a nearly identical global charge of ca. –0.7 to each Cp ring for the oxo and imido derivatives (whereas a difference is calculated by the Mulliken method). The Cp charge in the anionic methyne derivative is even closer to –1. In contrast, the Cp charge is much reduced for the cationic fluoro complex. An increasing ionic character may be deduced for the Ce–Cp interaction in the order F<sup>+</sup> < O  $\approx$  NH < CH<sup>-</sup>. The global negative charge on the Z group is also greatly reduced by the transfer of charge to the Ce<sup>4+</sup> ion, from the ideal ionic value of –1 for F, –2 for O and NH, and –3 for CH. The degree of charge transfer, and thereby the covalent contribution, increases in the order F<sup>-</sup> < O<sup>2-</sup>  $\approx$  NH<sup>2-</sup> < CH<sup>3-</sup>. In summary, there is an inverse relationship between the ionicity/covalency of the Ce–Cp and Ce–Z bonds: as the Ce–Cp bonds become more and more ionic, the Ce–Z bond correspondingly becomes more and more covalent. As a result, the metal effective charge is only slightly higher than +2 for all four compounds. This charge, however, is very substantially reduced from the theoretical ionic value of +4. For Ln(III) compounds with ligands of moderate electronegativity (e.g., the trialkyl and the tris(amido) compounds) the NBO charge on the Ln element, calculated at

(99) Clark, D. L.; Gordon, J. C.; Hay, P. J.; Martin, R. L.; Poli, R. *Organometallics* **2002**, *21*, 5000–5006.

(100) Perrin, L.; Maron, L.; Eisenstein, O. *Faraday Discuss.* **2003**, *124*, 25–39.

(101) Reed, A. E.; Curtiss, L. A.; Weinhold, F. *Chem. Rev.* **1988**, *88*, 899–926.



**Table 7. Natural Population of Atomic Orbitals for the Ce Atom in Compounds Cp<sub>2</sub>CeZ (Z = F<sup>+</sup>, O, NH, CH<sup>-</sup>) and for the Hf Atom in Cp<sub>2</sub>HfO**

compound	4f	5s	5p	5d	6s	6p
Cp <sub>2</sub> CeF <sup>+</sup>	1.04	2.00	5.98	0.41	0.07	0.00
Cp <sub>2</sub> CeO	1.01	1.99	5.93	0.45	0.09	0.03
Cp <sub>2</sub> Ce(NH)	1.09	1.99	5.95	0.41	0.00	0.01
Cp <sub>2</sub> Ce(CH <sup>-</sup> )	1.15	1.98	5.94	0.55	0.00	0.04
Cp <sub>2</sub> Ce(CH <sub>2</sub> )	1.15	1.99	5.96	0.42	0.00	0.01
Cp <sub>2</sub> Ce(CH <sub>2</sub> )(NH <sub>3</sub> )	1.18	1.99	5.96	0.42	0.00	0.01
Cp <sub>2</sub> HfO	[core]	2.00	5.99	1.71	0.13	0.00

comparable levels of theory, is *greater* than for the Ce(IV) compounds described here!<sup>34,35,102</sup> The significant participation of the 4f and 5d orbitals in bonding finds a rationalization in this exceptionally high (for lanthanide compounds) charge transfer, as indicated in the previous section.

It is interesting to note that the NBO charge on the Ce atom is only slightly lower in the methyne complex relative to the fluoro, oxo, and imido analogues, whereas there is a much bigger relative drop according to the Mulliken analysis. As discussed earlier, the MOs describing the Ce–CH  $\pi$  interactions are in fact at higher energy than the accepting orbitals of the Cp<sub>2</sub>Ce<sup>2+</sup> fragment, leading to the suggestion of a significant change of the electronic distribution for the Ce–Z triple bond. The trend of the metal Mulliken charges shows this redistribution more clearly than the trend of the corresponding NBO charges.

The natural population of the atomic orbitals in the various compounds is detailed in Table 7. The data further confirm the involvement of both the 4f and 5d orbitals in chemical bonding, the population always exceeding that of the free atom f<sup>1</sup> configuration. The 4f orbital population increases as the electronegativity of Z decreases, paralleling the increase of f contribution to the Ce–Z  $\pi$  bonding.

A final consideration concerns the expected reactivity of the four isoelectronic Cp<sub>2</sub>CeZ compounds examined in this section. The HOMO is a relatively low-energy Cp–Ce  $\pi$  combination with mostly Cp ligand character for Z = F<sup>+</sup>, O, and NH, and a relatively high-energy covalent Ce–Z  $\pi$  bonding combination when Z = CH<sup>-</sup>. The three former compounds should consequently be rather stable toward electrophilic reagents, whereas the carbyne system is expected to withstand facile electrophilic attacks at the Ce–C triple bond. A radical addition to the carbyne carbon, accompanied by an internal electron transfer to the metal center, should also result in the stabilization of the high-energy orbitals. The LUMO has a much lower energy for the fluoro complex than for the others. Consequently, the fluoro complex is expected to be much more likely to undergo nucleophilic addition and one-electron reduction processes. Ultimately, the oxo and imido complexes would seem to be the most susceptible systems to be stable in a chemical sense, and the imido system might represent a most suitable synthetic target given the additional steric protection provided by the N substituent. Adducts of these compounds with a neutral ligand, Cp<sub>2</sub>Ce(Z)(L), could also be accessible compounds, given

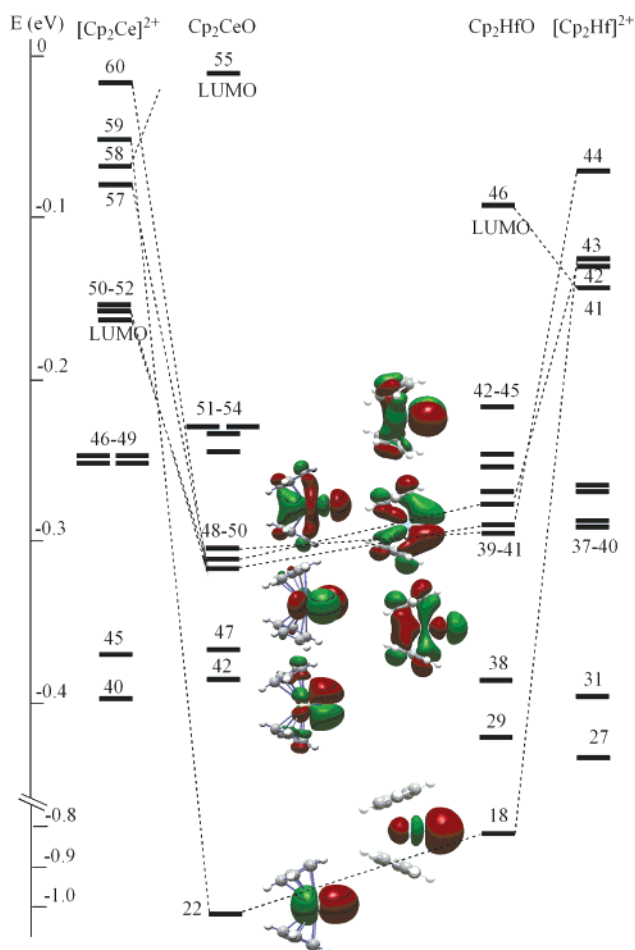


**Figure 4.** Energy diagram of the Kohn–Sham orbitals for the optimized Cp<sub>2</sub>MO structures (M = Ce, Hf), in comparison with the corresponding frozen Cp<sub>2</sub>M<sup>2+</sup> moieties. The orbital energies for the cationic species were scaled as for Figure 2.

the existence of compounds with the same stoichiometry for Hf.<sup>103</sup> Their formal 20-electron configuration when considering the Ce–Z bond as having bond order three would not introduce large instability, given the strong ionic character of the Ce–Cp interactions (see also the discussion on the Cp<sub>2</sub>Ce(CH<sub>2</sub>)(NH<sub>3</sub>) molecule below).

**Comparison between Cp<sub>2</sub>MO (M = Ce and Hf).** Before moving on to the alkylidene system, it is useful to compare the results of the calculations between related Ce<sup>4+</sup> and Hf<sup>4+</sup> system. In the Hf complexes, in which there is complete filling of the 4f subshell, only the 5d orbitals are available to accept charge from the ligands. Contrary to the essentially unexplored chemistry of Cp<sub>2</sub>Ce(IV) derivatives, Cp<sub>2</sub>Hf(IV) compounds are relatively well developed, and Lewis base adducts of ring-substituted Cp<sub>2</sub>HfO compounds, (C<sub>5</sub>Me<sub>4</sub>R)<sub>2</sub>Hf(O)-(py) (R = Me, Et), have been reported.<sup>103</sup> We have restricted our comparison to the representative case of the two oxo derivatives. The electronic structures of the two compounds and those of the parent [Cp<sub>2</sub>M]<sup>2+</sup> fragments are shown side by side in Figure 4. The optimized Cp<sub>2</sub>HfO structure (Hf–O, 1.80 Å; Hf–CNT, 2.30 Å; CNT–Hf–CNT', 124.6°) is close to that previously obtained at the RHF level (Hf–O, 1.76 Å; Hf–

(102) Brady, E. D.; Clark, D. L.; Gordon, J. C.; Hay, P. J.; Keogh, D. W.; Poli, R.; Scott, B. L.; Watkin, J. G. *Inorg. Chem.* **2003**, *42*, 6682–6690.

(103) Howard, W. A.; Parkin, G. *J. Organomet. Chem.* **1994**, *472*, C1–C4.

**Table 8. Percent Atomic Orbital Contribution to the MOs of Cp<sub>2</sub>HfO**

MO	<i>E</i> (eV)	Hf			O		C
		s	p	d	s	p	
46 (LUMO), b <sub>1</sub>	-0.092	23.5	0.0	63.0	0.1	0.9	12.6
45 (Hf–Cp π), b <sub>2</sub>	-0.214					29.4	70.2
44 (Hf–Cp π), a <sub>1</sub>	-0.247	0.9	1.9	8.0	1.2	40.1	47.8
43 (Hf–Cp π), b <sub>1</sub>	-0.255		10.8			13.0	76.2
42 (Hf–Cp π), a <sub>2</sub>	-0.270			19.9			79.6
41 (Hf–O π), b <sub>2</sub>	-0.278		0.3	27.6		59.6	12.6
40 (Hf–O π), b <sub>1</sub>	-0.288		3.2	22.5		48.7	25.4
39 (Hf–O σ), a <sub>1</sub>	-0.293		4.0	20.1	2.3	34.2	39.1
38 (Hf–Cp σ), b <sub>2</sub>	-0.386		6.4	1.4			88.4
29 (Hf–Cp σ), a <sub>1</sub>	-0.423	8.2	1.4	1.6			69.8
18 (O 2s), a <sub>1</sub>	-0.821	1.4	3.3	4.0	89.4	0.8	1.2

CNT, 2.31 Å; CNT–Hf–CNT<sup>+</sup>, 131°).<sup>104</sup> In particular, the Hf–O bond distance is closer to that experimentally determined in the above-mentioned pyridine adduct (1.826(9)°).<sup>103</sup>

Relative to [Cp<sub>2</sub>Ce]<sup>2+</sup>, the structure of [Cp<sub>2</sub>Hf]<sup>2+</sup> is simplified by the absence of the 4f orbitals from the frontier region. The frontier accepting orbitals in the wedge plane for the hafnium fragment (nos. 41–44 in the right column of Figure 4) follow the expected trend. Upon binding the O<sup>2-</sup> ion, orbital 43 (2a<sub>1</sub>) is used to establish the σ bond, whereas orbitals 42 (b<sub>1</sub>) and 44 (b<sub>2</sub>) are used to establish the π<sub>⊥</sub> and π<sub>||</sub> interactions, respectively. The 1a<sub>1</sub> orbital (no. 41) becomes the LUMO in the oxo derivative.

With only few very important exceptions, the orbital energies are lower, a clear consequence of the lanthanide contraction, for the Hf species relative to the orbitals in the corresponding Ce species. Whereas the Ce–Cp π bonding orbitals for Cp<sub>2</sub>CeO are grouped in a narrow energy region, the same orbitals are more spread out for the related Hf compound, with the highest energy one (no. 45) ending up at a higher energy than for Ce. The reason for this behavior can be traced to a greater mixing between the oxygen p<sub>||</sub> orbital and the appropriate out-of-phase combination of the two ring Huckel-type π<sub>2</sub> orbitals. This mixing, which is out-of-phase (and mostly ring based) in orbital no. 45, has a destabilizing effect on this orbital, whereas the corresponding in-phase (and mostly O 2p) mixing stabilizes orbital no. 40. The most notable exceptions, however, are the M–O σ and π bonding orbitals. The former is almost 2 eV higher in energy for Hf. A possible reason for this trend is a stronger σ overlap (and also a slightly better energy match) between the oxygen donor orbitals and the more expanded acceptor orbitals of the [Cp<sub>2</sub>Ce]<sup>2+</sup> moiety. M–O π bonding appears to be more covalent for the Hf compound than the Ce compound. In Table 8 we note that the Hf–O π bonding orbitals have substantial d character (22–28%) compared to the corresponding orbitals in Cp<sub>2</sub>CeO, where there was significantly less d character (10–15%) but some f character (8%). This is also reflected in Table 7, by comparing the 5d population of Cp<sub>2</sub>HfO of 1.71 with that of Cp<sub>2</sub>CeO of 0.45.

The NBO charges for the two oxo compounds are compared in Table 6. They show, as expected, that the O and Cp ligands transfer a greater amount of charge to the metal center in the Hf compound, indicating that

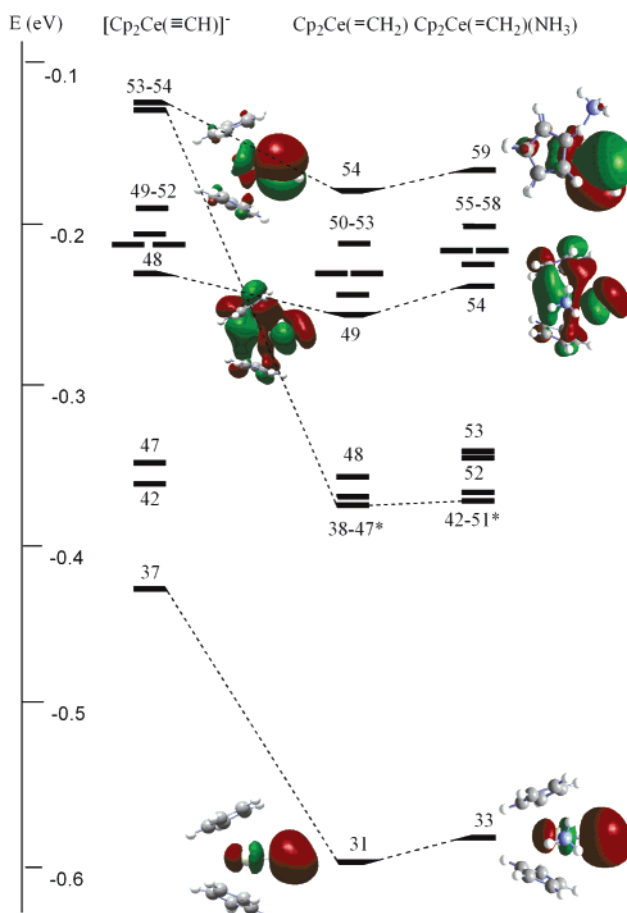


**Figure 5.** Energy diagram of the Kohn–Sham orbitals for the optimized Cp<sub>2</sub>Ce(CH<sub>2</sub>) and Cp<sub>2</sub>Ce(CH<sub>2</sub>)(NH<sub>3</sub>) structures and relationship to the energy diagram of [Cp<sub>2</sub>Ce(CH)]<sup>-</sup>. For the MOs indicated as a starred range, see text.

the Hf compound is more covalent than the Ce analogue. Thus, the ionic component of the M–O bond is greater for Ce and smaller for Hf. However, the effective charge on Hf, 2.058, is not tremendously lower than the effective charge carried by the Ce atom, 2.421, in the related compound. The strong covalency in both Ce and Hf systems is also clearly reflected by the natural population analysis of Table 7.

The Mulliken analysis, on the other hand, attributes a lower positive charge to the Ce atom and correspondingly lower negative charges to all ligands in the Ce complex. This difference could result from an overestimation by the Mulliken analysis of the charge transferred in the Ce system, due to the explicit inclusion of the f orbitals in the calculation.

**Electronic Structure of the Methylene Complexes.** Figure 5 shows the relationship between the Kohn–Sham orbitals of complex Cp<sub>2</sub>Ce(CH)<sup>-</sup> and those of its protonation product, the carbene complex Cp<sub>2</sub>Ce(CH<sub>2</sub>), and the NH<sub>3</sub> addition product of the latter, Cp<sub>2</sub>Ce(CH<sub>2</sub>)(NH<sub>3</sub>). From first principles, one might expect that the Ce–C triple (σ+2π) bond should reduce to a double bond upon protonating the carbyne ligand. This is indeed what happens. The planar Ce–CH<sub>2</sub> moiety is slightly tilted relative to the Cp<sub>2</sub>Ce wedge plane, and the residual π bonding orbital is placed perpendicularly to this plane as expected (orbital 54 in the central diagram of Figure 5). This orbital is found at lower

(104) Benson, M.; Cundari, T.; Lim, S.; Nguyen, H.; Piercebeaver, K. *J. Am. Chem. Soc.* **1994**, *116* (9), 3955–3966.

energy relative to the situation in the parent carbyne complex, possibly because of the increased effective metal charge (see Table 6). The other Ce–C (carbyne)  $\pi$  bonding orbital is replaced in the carbene species by a deeper orbital, which is part of the orbital group marked as 38–47\* in Figure 5. Because of the energy proximity and the low symmetry, the newly formed C–H interaction mixes with the Cp C–H and C–C bonding orbitals in several molecular orbitals. This mixing renders a detailed analysis of the bonding, in particular the  $\alpha$ -agostic Ce $\cdots$ H interaction, difficult. At any rate, it is clear that the direct participation of metal orbitals is responsible for the peculiar Ce=CH<sub>2</sub> geometry (vide supra). The Ce–Cp  $\sigma$  interactions (one of them being also mixed in the 38–47\* orbital group, the other being orbital 48) and the Ce–Cp  $\pi$  interactions (orbitals 50–53) are also found at lower energy with respect to the parent carbyne complex, a fact that is again attributed to the increased effective metal charge. The shape of the Ce–Cp  $\sigma$  orbitals (not shown) and composition are very similar to the situation in the parent carbyne complex.

The addition of an ammonia molecule to the carbene complex introduces only minor changes in the system molecular orbital energies, as can be appreciated from Figure 5. The overall trend is a slight energy increase with respect to the NH<sub>3</sub>-free carbene complex, in line with the slight decrease of effective metal charge (see Table 6). The main point of interest is that the  $\alpha$ -agostic Ce $\cdots$ H interaction is not lost upon addition of the NH<sub>3</sub> ligand. As mentioned in the geometry section above, this compound has a formal electron count of 20 when considering the two additional electrons provided by the NH<sub>3</sub> ligand and the agostic interaction. This unusual behavior (as compared with the d elements, which cannot expand their number of valence electrons beyond 18) can be rationalized on the basis of the previous observation of mainly covalent interactions in the wedge plane and mainly ionic interactions perpendicular to this plane (e.g., the Ce–Cp  $\sigma$  interactions). Thus, the system prefers to establish the new bond with NH<sub>3</sub> and keep the  $\alpha$ -agostic bond, at the expense of the Ce–Cp  $\sigma$  interactions, which consequently become even more ionic with respect to the Ce–Cp interactions. This view is in line with several observations: (i) the NBO charge on the two Cp ligands increases from –1.397 to –1.417 upon NH<sub>3</sub> addition, see Table 6; (ii) the Ce–CNT distances correspondingly increase upon NH<sub>3</sub> addition, see Table 1; (iii) the Ce–Cp  $\sigma$  bonding orbitals in compound Cp<sub>2</sub>Ce(CH<sub>2</sub>)(NH<sub>3</sub>) (orbitals 52 and 53) increase in energy by a greater amount than the other orbitals, relative to the NH<sub>3</sub>-free complex. The energetic gain associated with the NH<sub>3</sub> coordination (i.e., the Ce–NH<sub>3</sub> bond dissociation energy) is 26.3 kcal/mol, leading to the prediction that NH<sub>3</sub> will be weakly bonded to the metal center. The possibility of Ce complexes with formal electron counts higher than 18 could also be achieved in principle by use of the additional acceptor orbitals available within the 4f and 5d shells. However, in comparing the natural populations of atomic orbitals on Ce in Cp<sub>2</sub>Ce(CH<sub>2</sub>) and Cp<sub>2</sub>Ce(CH<sub>2</sub>)(NH<sub>3</sub>), one sees virtually no change in the 4f and 5d populations.

## Conclusions

The main result of the present computational study is the recognition that species with terminal multiple bonds between lanthanide ions (such as tetravalent cerium) and main group elements appear to be legitimate synthetic targets. The ability of transition metal complexes supporting these general functionalities to undergo a wide range of reactivity (e.g., metathesis of imines, aldehydes, and carbodiimides, metallacycle formation with alkenes and alkynes, and dealkylation and C–H bond activation chemistry) is well documented.<sup>105–114</sup> Thus, we suggest that a similarly rich chemistry should be accessible for the 4f element analogues.

In our computational study we find some rather fascinating fundamental differences in the nature of M–O bonding interactions between the transition metal and lanthanide systems. For Hf, the M–O  $\sigma$  bonding can be traced primarily to one bonding orbital that is best described as a combination of O 2p with a Hf p–d hybrid. For Ce, this interaction is split between two orbitals, both of which are quite covalent in nature. The lower lying orbital is primarily a mixture of O 2s with Ce p, while the higher energy combination is best described as a mixture of O 2p with a Ce p–d–f hybrid. The M–O  $\pi$  bonding interactions result from O 2p interactions with either Hf 5d or a combination of Ce 5d/4f. The greater participation of the metal 5d orbitals in the Hf–O  $\pi$  bonds points to stronger  $\pi$  bonding for the Hf compound. The overall situation would appear to be one of stronger  $\sigma$  bonding in the lanthanide system and stronger  $\pi$  bonding in the transition metal system. In this regard, there is a striking similarity in M–O  $\sigma$  bonding in the [CeO<sup>2+</sup>] core and the more familiar [UO<sub>2</sub><sup>2+</sup>] core in actinide systems. The uranyl U–O  $\sigma$  bonding has been shown to be derived from a unique p–f hybridization, and the resulting U–O  $\sigma$  bonding is incredibly strong.<sup>28</sup>

A question that immediately comes to mind in the case of the 4f elements is that if these bonds are predicted to be reasonably stable, then why have compounds exhibiting them not yet been isolated and characterized? In terms of the relevant bonding interactions studied here, while displaying a reasonably strong covalent component, these remain nevertheless quite polarized interactions, with all associated reactivity problems, especially the hydrolytic sensitivity of the carbon-based ligands. In addition, aggregation to oligonuclear species is always a potential problem in lanthanide chemistry. Although most of the attention has

(105) Zuckerman, R. L.; Krska, S. W.; Bergman, R. G. *J. Am. Chem. Soc.* **2000**, *122*, 751.

(106) Birdwhistell, K. R.; Lanza, J.; Pasos, J. *J. Organomet. Chem.* **1999**, *584*, 200.

(107) Polse, J. L.; Andersen, R. A.; Bergman, R. G. *J. Am. Chem. Soc.* **1998**, *120*, 13405.

(108) Lee, S. Y.; Bergman, R. G. *Tetrahedron* **1995**, *51*, 4255.

(109) Mcgrane, P. L.; Jensen, M.; Livinghouse, T. *J. Am. Chem. Soc.* **1992**, *114*, 5459.

(110) Blake, R. E.; Antonelli, D. M.; Henling, L. M.; Schaefer, W. P.; Hardcastle, K. I.; Bercaw, J. E. *Organometallics* **1998**, *17*, 718.

(111) Walsh, P. J.; Hollander, F. J.; Bergman, R. G. *J. Am. Chem. Soc.* **1988**, *110*, 8729.

(112) Gade, L. H.; Mountford, P. *Coord. Chem. Rev.* **2001**, *216–217*, 65.

(113) Duncan, A. P.; Bergman, R. G. *Chem. Rec.* **2002**, *2*, 431.

(114) Wang, W. D.; Espenson, J. H. *Organometallics* **1999**, *18*, 5170.



been devoted to the synthesis, structure, and reactivity of Ln(III) and Ln(II) compounds, cyclopentadienyl derivatives have also been proven to exist for the +4 oxidation state.<sup>36–45</sup> These systems, or analogues with more sterically encumbered cyclopentadienyl rings, could therefore provide access to the target compounds. The field of chemistry has provided many examples of reactive transition metal complexes whose chemistry has languished when the heavier congeners of the series have been targeted. For example, the dimolybdenum-(II) tetracarboxylate  $\text{Mo}_2(\text{O}_2\text{CCH}_3)_4$  was first synthesized by Wilkinson and co-workers in 1964.<sup>115</sup> Following similar synthetic routes, the heavier tungsten analogue,  $\text{W}_2(\text{O}_2\text{CCH}_3)_4$ , proved difficult to isolate.<sup>116–119</sup> A recognition of the differing chemical properties of tungsten compared to molybdenum eventually led to the preparation of the ditungsten derivative, albeit 17 years later.<sup>120</sup> With this in mind, we are currently developing new approaches toward the isolation of novel examples of compounds containing Ln=Z multiple bonds. We envision that these systems not only will provide us with new and interesting insights into the structure and bonding of the f elements but may also constitute

(115) Stephenson, T. A.; Bannister, E.; Wilkinson, G. *J. Chem. Soc.* **1964**, 2538.

(116) Cotton, F. A.; Koch, S.; Mertis, K.; Millar, M.; Wilkinson, G. *J. Am. Chem. Soc.* **1977**, *99*, 4989.

(117) Bino, A.; Cotton, F. A.; Dori, Z.; Koch, S.; Kuppers, H.; Millar, M.; Sekutowski, J. C. *Inorg. Chem.* **1978**, *17*, 3245.

(118) Cotton, F. A.; Fanwick, P. E.; Niswander, R. H.; Sekutowski, J. C. *J. Am. Chem. Soc.* **1978**, *100*, 4725.

(119) Sharp, P. R.; Schrock, R. R. *J. Am. Chem. Soc.* **1980**, *102*, 1430–1431.

(120) Sattelberger, A. P.; Mclaughlin, K. W.; Huffman, J. C. *J. Am. Chem. Soc.* **1981**, *103*, 2880.

potentially reactive systems with which to carry out a broad range of small molecule transformations.

**Note Added in Proof.** In the NBO analysis we note that the 6s and 4f orbitals are treated as valence orbitals, while the 6p and 5d orbitals partitioned as Rydberg orbitals. The effective charges obtained using this standard NBO approach in Table 6 may be smaller than when the 5d orbital is included as a valence orbital. The Mulliken analysis in Tables 2–5 shows strong 5d participation. Modification of the NBO procedure results in reduced atomic charges by including the 4p orbital in the valence set in first-row transition metal complexes<sup>121</sup> and the 6d orbital in the valence set in actinide complexes.<sup>122</sup>

**Acknowledgment.** R.P. is grateful to CINES (Montpellier, France) and the CICT (preject CALMIP, Toulouse, France) for granting free computer time, and to the G. T. Seaborg Institute for sponsoring a stay at Los Alamos National Laboratory (July–August 2002). J.C.G. and P.J.H. acknowledge support from the Laboratory Directed Research and Development program at Los Alamos National Laboratory. D.L.C. acknowledges support from the Office of Basic Energy Science, Division of Chemical Sciences, U.S. Department of Energy. Los Alamos National Laboratory is operated by the University of California for the U.S. Department of Energy under Contract W-7405-ENG-36.

OM050693Y

(121) Maseras, F.; Morokuma, K. *Chem. Phys. Lett.* **1992**, *195*, 500.

(122) Clark, A. E.; Sonnenberg, J. L.; Hay, P. J.; Martin, R. L. *J. Chem. Phys.* **2004**, *121*, 2144.